

E4-2004-131

I. V. Titkova, V. A. Bednyakov

NEUTRALINO–NUCLEON CROSS SECTIONS
FOR DETECTION OF LOW-MASS DARK
MATTER PARTICLES

Presented at the school IS CRA, 14th Course «Neutrinos and Explosive
Events in the Universe», Erice, Italy, July 2–13, 2004.

Титкова И. В., Бедняков В. А.

E4-2004-131

Сечения взаимодействия нейтралино с нуклонами
для детектирования легких частиц темной материи

Одними из главных кандидатов на роль темной материи являются слабо-взаимодействующие массивные частицы (WIMP). В рамках эффективной низкоэнергетичной суперсимметричной стандартной модели для относительно малых масс нейтралино (в роли WIMP) были рассчитаны сечения спинзависимого и скалярного взаимодействий нейтралино с ядрами. Проведено сравнение результатов расчетов с экспериментальными данными для WIMP-протонных и WIMP-нейтронных сечений взаимодействия. Показано, что для достижения теоретических предсказаний необходимо увеличение чувствительности эксперимента примерно в 50–100 раз. Для корректного сравнения данных необходимо использовать смешанный спин-скалярный подход. Исходя из данных эксперимента DAMA в рамках эффективной суперсимметричной стандартной модели следует ожидать легкий сектор бозонов Хиггса, достаточно высокую скорость счета событий для детектора из ^{73}Ge , а также значительный поток мюонов от аннигиляции нейтралино на Земле и Солнце.

Работа выполнена в Лаборатории ядерных проблем им. В. П. Дзелепова ОИЯИ.

Препринт Объединенного института ядерных исследований. Дубна, 2004

Titkova I. V., Bednyakov V. A.

E4-2004-131

Neutralino–Nucleon Cross Sections for Detection
of Low-Mass Dark Matter Particles

The weakly interacting massive particle (WIMP) is one of the main candidates for the relic dark matter. In the effective low-energy minimal supersymmetric standard model (effMSSM), the neutralino–nucleon spin and scalar cross sections in the low-mass regime were calculated. The calculated cross sections are compared with almost all currently available experimental exclusion curves for spin-dependent WIMP–proton and WIMP–neutron cross sections. It is demonstrated that in general about two-orders-of-magnitude improvement of the current DM experimental sensitivities is needed to reach the effMSSM SUSY predictions. To avoid misleading discrepancies between data and SUSY calculations, it is preferable to use a mixed spin-scalar coupling approach. It is noticed that the DAMA evidence favours the light Higgs sector in the effMSSM, a high event rate in a ^{73}Ge detector and relatively high ongoing muon fluxes from relic neutralino annihilations on the Earth and the Sun.

The investigation has been performed at the Dzhelepov Laboratory of Nuclear Problems, JINR.

Preprint of the Joint Institute for Nuclear Research. Dubna, 2004

INTRODUCTION

The weakly interacting massive particle (WIMP) is one of the main candidates for the relic dark matter (DM). The lightest supersymmetric particle (LSP), the lightest neutralino, is assumed to be the best WIMP DM candidate. It is believed that for heavy nuclei the spin-independent (SI) interaction gives the dominant contribution to the expected event rate of its detection. The results obtained are usually presented in the form of exclusion curves due to non-observation of the WIMPs. For fixed mass of the WIMP the cross sections located above these curves are excluded.

Only the DAMA collaboration claims observation of the first evidence for the DM signal due to registration of the annual modulation effect [1–3]. The DAMA results are shown in Fig. 1, where the contour lines for some present experimental limits (solid lines) and for some projected experiments (dashed lines) are presented. The closed DAMA contour corresponds to a complete neglecting of the spin-dependent (SD) interaction, open contour is obtained with the assumption that the SD cross section equals 0.08 pb [2].

The main result of the DAMA experiment is the low-mass region of the WIMP mass ($40 < m_\chi < 150$ GeV), provided these WIMPs are cold dark matter particles. It is obvious that such serious claim should be verified by another completely independent experiment. This mission could be expected by new generation experiments with large mass of Ge detector both with spin (^{73}Ge) and spinless (natural Ge). A new set-up (GENIUS-TF) has already been installed and works in Gran Sasso Laboratory [4]. This experiment is planned to be sensitive to the annual modulation signal with data taking over about five years with a large mass of the Ge detectors [5].

There are three reasons to think that the SD interaction could be very important:

- SI interactions give only one constraint for SUSY models, while the SD interactions give two constraints [6];
- even with very sensitive detector, which is sensitive only to SI interaction, one can miss a DM signal;
- a complicated nuclear spin structure possesses the long-tail form-factor behaviour. For heavy-mass target nuclei and heavy WIMP masses the SD efficiency to detect a DM signal is much higher than the SI efficiency [7].

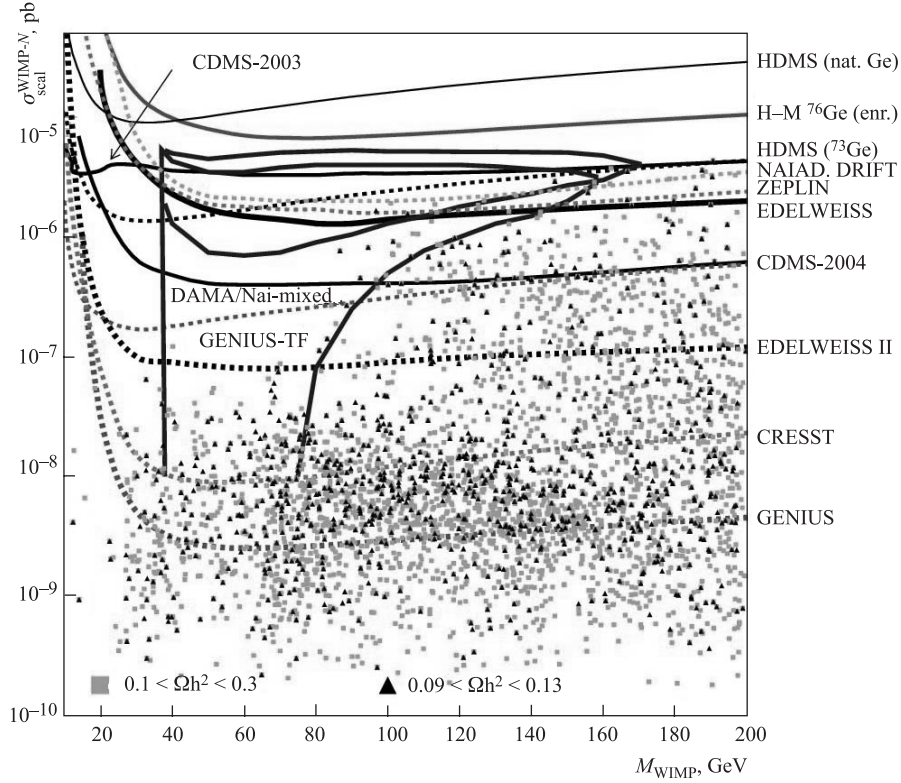


Fig. 1. WIMP–nucleon cross section limits for spin-independent interactions for present and projected experiments and our theoretical expectation (scatter plots)

In this paper we consider some aspects of the SD and SI interactions and some consequences of the DAMA results (more information can be found in [8]).

1. THEORETICAL APPROACH

The WIMP–nucleus elastic cross section depends on the WIMP–quark interaction strength, the distribution of quarks in nucleon and nucleons in nucleus plays a crucial role. Thus the calculation of WIMP–nucleus interaction must take place in three steps:

1) Calculations of the WIMP interactions with quarks and gluons. The couplings of the neutralino with all six quarks and gluons as well as the masses of the exchanged particles are defined by the parameters of a SUSY model.

2) Translation of the microscopic interaction into the interactions with nucleons.

3) Using nuclear wave functions, spin and scalar components of the nucleons must be added coherently to give the matrix element for the WIMP–nucleus cross section as a function of momentum transfer.

An important simplification of these calculations occurs because the elastic scattering takes place in the nonrelativistic limit. So generally, only two cases need to be considered: the spin–spin interaction and scalar interaction. Therefore, the elastic-scattering cross section is the sum of these two pieces.

1.1. Feynman Rules and Effective Lagrangian. We will use the minimal supersymmetric (SUSY) extension of the standard model (MSSM). This is a group of models, which contains the minimum number of new particles and has all possible CP-conserving soft supersymmetry-breaking terms in the Lagrangian. There are four neutralinos in MSSM, which are linear combinations of the supersymmetric partners of the neutral gauge bosons, and two Higgs bosons. The lightest neutralino (LSP) is stable, we denote it by $\chi = N_{11}\tilde{B} + N_{12}\tilde{Z} + N_{13}\tilde{H}_1^0 + N_{14}\tilde{H}_2^0$. The Feynman diagrams, which give rise to the neutralino–quark axial-vector and scalar interactions, are presented in Figs. 2 and 3. More details

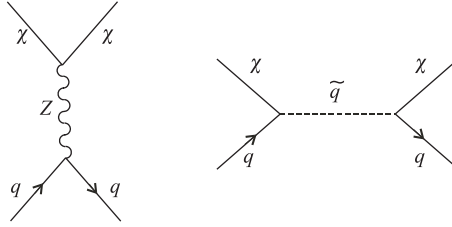


Fig. 2. Feynman diagrams contributing to the spin-dependent elastic scattering of neutralinos from quarks

on the Feynman rules and techniques for handling Majorana fermions can be found in [9, 10]. We use only results of these calculations.

The interaction of the Z boson with quarks are described by the same Lagrangian as given in the Standard Model (SM):

$$L_{Zqq} = \frac{g}{\sin \theta_w \cos \theta_w} \bar{q} \gamma_\mu [(Q_q \sin^2 \theta_w - T_3) P_L + Q_q \sin^2 \theta_w P_R] q Z^\mu,$$

where Q_q is the quark charge, $P_{R,L} = \frac{1}{2}(1 \pm \gamma_5)$, T_3 is the quark isospin, θ_w is Weinberg angle.

The $Z\chi\chi$ vertex is as follows: $\frac{ig}{2 \cos \theta_w} \gamma^\mu [O''_{ij}{}^L (1 - \gamma_5) + O''_{ij}{}^R (1 + \gamma_5)]$,

where $O''_{ij}{}^L = -\frac{1}{2} N_{i3} N_{j3}^* + \frac{1}{2} N_{i4} N_{j4}^*$, $O''_{ij}{}^R = -O''_{ij}{}^L$, N is the matrix, which diagonalizes the neutralino mass matrix

$$M_\chi = \begin{pmatrix} M_1 & 0 & -m_z \cos \beta \sin \theta_w & m_z \sin \beta \sin \theta_w \\ 0 & M_2 & m_z \cos \beta \cos \theta_w & -m_z \sin \beta \cos \theta_w \\ -m_z \cos \beta \sin \theta_w & m_z \cos \beta \cos \theta_w & 0 & -\mu \\ m_z \sin \beta \sin \theta_w & -m_z \sin \beta \cos \theta_w & -\mu & 0 \end{pmatrix},$$

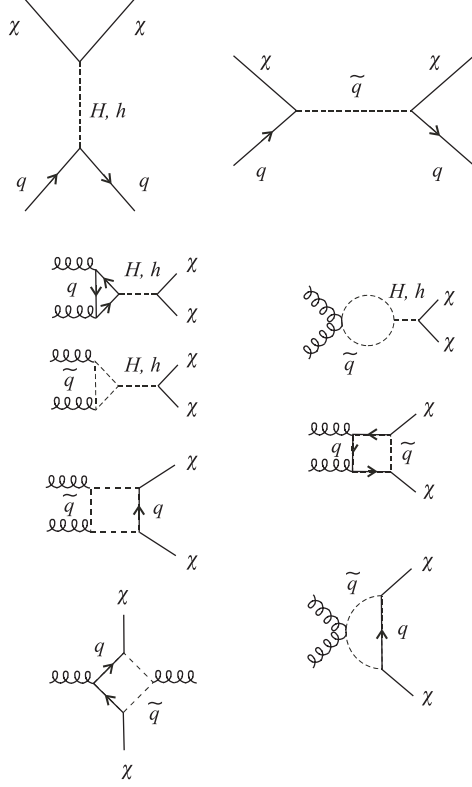


Fig. 3. Feynman diagrams contributing to the scalar elastic-scattering amplitude of the neutralinos from quarks (top) and to the gluonic interaction with neutralinos

where $\text{tg } \beta = \frac{v_2}{v_1}$ is the ratio of the vacuum expectation values, m_z is the mass of the Z boson, $M_{1,2}$ are soft gaugino mass parameters, μ is Higgs mass parameter (these parameters are dependent on a SUSY model). The Lagrangian for $Z\chi\chi$ vertex (taking into account the fact that neutralino is Majorana particle) is as follows:

$$L_{Z\chi\chi} = \frac{g}{4 \sin \theta_w \cos \theta_w} \left[|N_{13}|^2 - |N_{14}|^2 \right] (\bar{\chi} \gamma^\mu \gamma_5 \chi) Z_\mu.$$

The interactions of the neutral Higgs bosons with quarks are described by the Lagrangian

$$L_{H_k q q} = -\frac{h_d}{\sqrt{2}} \bar{d} [Q_{2k} + iQ_{1k} \sin \beta \gamma_5] d H_k - \frac{h_u}{\sqrt{2}} \bar{u} [Q_{3k} + iQ_{1k} \cos \beta \gamma_5] u H_k,$$

where the Yukawa couplings of down- and up-quarks are given by $h_d = \frac{gm_d}{\sqrt{2} \sin \theta_w m_Z \cos \beta}$, and $h_u = \frac{gm_u}{\sqrt{2} \sin \theta_w m_Z \sin \beta}$, matrix Q is 3×3 rotation matrix, which diagonalizes the Higgs-mass matrix.

The interaction of the lightest neutralino with pair quark-squark comes from both gauge and Yukawa interactions. After coinciding the general flavour-diagonal squark mixing as well as neutralino mixing, the following Lagrangian is obtained:

$$L_{\chi q \bar{q}} = -\frac{g}{\sqrt{2} \sin \theta_w} [\tilde{q}_1^* \bar{\chi} (B_q^{1L} P_L + B_q^{1R} P_R) q + (1 \rightarrow 2)].$$

$B_q^{iL,R}$ is the mass eigenstate basis, expressed for the squark mixing angle θ_q and phase ϕ_q :

$$\begin{aligned} B_q^{1L} &= \cos \theta_q A_q^{LL} + e^{-i\phi_q} \sin \theta_q A_q^{RL}, & B_q^{2L} &= \cos \theta_q A_q^{RL} - e^{i\phi_q} \sin \theta_q A_q^{LL}, \\ B_q^{1R} &= \cos \theta_q A_q^{LR} + e^{-i\phi_q} \sin \theta_q A_q^{RR}, & B_q^{2R} &= \cos \theta_q A_q^{RR} - e^{i\phi_q} \sin \theta_q A_q^{LR}. \end{aligned}$$

Here A for up-type quarks may be written as

$$\begin{aligned} A_u^{LL} &= N_{12}^* + \frac{1}{3} \text{tg } \theta_w N_{11}^*, & A_u^{LR} &= \frac{\sqrt{2}}{g} \sin \theta_w h_u N_{14}, \\ A_u^{RL} &= \frac{\sqrt{2}}{g} \sin \theta_w h_u N_{14}^*, & A_u^{RR} &= \frac{4}{3} \text{tg } \theta_w N_{11} \end{aligned}$$

and for the down-types quarks as

$$\begin{aligned} A_d^{LL} &= -N_{12}^* + \frac{1}{3} \text{tg } \theta_w N_{11}^*, & A_d^{LR} &= \frac{\sqrt{2}}{g} \sin \theta_w h_d N_{13}, \\ A_d^{RL} &= \frac{\sqrt{2}}{g} \sin \theta_w h_d N_{13}^*, & A_d^{RR} &= \frac{2}{3} \text{tg } \theta_w N_{11} \end{aligned}$$

$A_q^{LL,RR}$ and $A_q^{LR,RL}$ originate from gauge and Yukawa interactions, respectively.

The Higgs-boson interactions with neutralinos are fixed by SUSY and gauge symmetry. There are five physical Higgs states: h^0 , H^0 , H^\pm , A^0 . The neutral CP-even states h^0 and H^0 are the mixtures of the neutral components of the interaction-state Higgs field. The mixing angle α is defined by: $\sin 2\alpha = -\sin 2\beta \left(\frac{m_H^2 + m_h^2}{m_H^2 - m_h^2} \right)$, $\cos 2\alpha = -\cos 2\beta \left(\frac{m_A^2 - m_Z^2}{m_H^2 - m_h^2} \right)$. Lagrangians of $H\chi\chi$ vertex are the following:

$$\begin{aligned} L_{H^0\chi\chi} &= \frac{1}{2} g H^0 \bar{\chi}_n [T_{Hnm}^* P_L + T_{Hnm} P_R] \chi_m, \\ L_{h^0\chi\chi} &= \frac{1}{2} g h^0 \bar{\chi}_n [T_{hnm} P_L + T_{hnm} P_R] \chi_m, \\ L_{A^0\chi\chi} &= \frac{1}{2} i g A^0 \bar{\chi}_n [-T_{Anm} P_L + T_{Anm} P_R] \chi_m, \end{aligned}$$

where

$$\begin{aligned}
T_{Hnm} &= -\cos\alpha R''_{nm} + \sin\alpha S''_{nm}, \\
T_{hnm} &= \sin\alpha R''_{nm} + \cos\alpha S''_{nm}, \\
T_{Anm} &= -\sin\beta R''_{nm*} + \cos\beta S''_{nm*}, \\
R''_{nm} &= \frac{1}{2}N_{3n}(N_{2m} - \text{tg}\theta_w N_{1m}) + (n \rightarrow m), \\
S''_{nm} &= \frac{1}{2}N_{4n}(N_{2n} - \text{tg}\theta_w N_{1m}) + (n \rightarrow m).
\end{aligned}$$

The effective low-energy Lagrangian of the axial-vector and scalar interactions of neutralino with quarks is given by

$$L_{\text{eff}} = A_q \bar{\chi} \gamma_\mu \gamma_5 \chi \cdot \bar{q} \gamma^\mu \gamma_5 q + C_q \bar{\chi} \chi \cdot q \bar{q}.$$

In the case of nonrelativistic neutralino the terms with vector and pseudoscalar quark currents are negligible (the typical relic neutralino velocity is $10^{-3} c$). The effective neutralino–quark axial-vector and scalar couplings are

$$\begin{aligned}
A_q &= -\frac{g^2}{4m_Z^2} \left[\frac{N_{14}^2 - N_{13}^2}{2} T_3 - \frac{m_Z^2}{m_{\tilde{q}_1}^2 - (m_\chi + m_q)^2} (\cos^2 \theta_q \phi_{qL}^2 + \sin^2 \theta_q \phi_{qR}^2) - \right. \\
&\quad \left. - \frac{m_Z^2}{m_{\tilde{q}_2}^2 - (m_\chi + m_q)^2} (\sin^2 \theta_q \phi_{qL}^2 + \cos^2 \theta_q \phi_{qR}^2) - \right. \\
&\quad \left. - \frac{m_q^2}{4} P_q \left(\frac{1}{m_{\tilde{q}_1}^2 - (m_\chi + m_q)^2} + \frac{1}{m_{\tilde{q}_2}^2 - (m_\chi + m_q)^2} \right) - \right. \\
&\quad \left. - \frac{m_q}{2} m_Z P_q \sin 2\theta_q T_3 (N_{12} - \text{tg}\theta_w N_{11}) \times \right. \\
&\quad \left. \times \left(\frac{1}{m_{\tilde{q}_1}^2 - (m_\chi + m_q)^2} + \frac{1}{m_{\tilde{q}_2}^2 - (m_\chi + m_q)^2} \right) \right],
\end{aligned}$$

where

$$\begin{aligned}
P_q &= \left(\frac{1}{2} + T_3 \right) \frac{N_{14}}{\sin\beta} + \left(\frac{1}{2} - T_3 \right) \frac{N_{13}}{\cos\beta}, \\
\phi_{qL} &= N_{12} T_3 + N_{11} (Q - T_3) \text{tg}\theta_w, \quad \phi_{qR} = N_{11} Q \text{tg}\theta_w,
\end{aligned}$$

and

$$\begin{aligned}
C_q = & -\frac{m_q}{m_Z} \cdot \frac{g^2}{4} \left[\frac{F_h}{m_h^2} h_q + \frac{F_H}{m_H^2} H_q + \left(\frac{m_q}{4m_Z} P_q^2 - \frac{m_Z}{m_q} \phi_{qL} \phi_{qR} \right) \times \right. \\
& \times \left(\frac{\sin 2\theta_q}{m_{\tilde{q}_1}^2 - (m_\chi + m_q)^2} - \frac{\sin 2\theta_q}{m_{\tilde{q}_2}^2 - (m_\chi + m_q)^2} \right) + \\
& \left. + P_q \left(\frac{\cos^2 \theta_q \phi_{qL} - \sin^2 \theta_q \phi_{qR}}{m_{\tilde{q}_1}^2 - (m_\chi + m_q)^2} - \frac{\cos^2 \theta_q \phi_{qR} - \sin^2 \theta_q \phi_{qL}}{m_{\tilde{q}_2}^2 - (m_\chi + m_q)^2} \right) \right],
\end{aligned}$$

where

$$\begin{aligned}
F_h &= (N_{12} - N_{11} \operatorname{tg} \theta_w) (N_{14} \cos \alpha + N_{13} \sin \alpha), \\
F_H &= (N_{12} - N_{11} \operatorname{tg} \theta_w) (N_{14} \sin \alpha + N_{13} \cos \alpha), \\
h_q &= \left(\frac{1}{2} + T_3 \right) \frac{\cos \alpha}{\sin \beta} - \left(\frac{1}{2} - T_3 \right) \frac{\sin \alpha}{\cos \beta}, \\
H_q &= \left(\frac{1}{2} + T_3 \right) \frac{\sin \alpha}{\sin \beta} - \left(\frac{1}{2} - T_3 \right) \frac{\cos \alpha}{\cos \beta}.
\end{aligned}$$

The coefficient A_q contains the Z -exchange contribution as well as the squark exchange, while the coefficient C_q has the Higgs-exchange contributions as well as the squark-exchange contribution (see Fig. 3).

1.2. Cross Section. The effective Lagrangian can be used for calculating the cross section of the scattering of the neutralino off heavy nucleus. We need detailed information about the configuration of protons and neutrons inside each nucleus and that of quarks and gluons inside each proton and neutron. In this work we will not touch on this issue in detail, the information about nuclei and parameterizations of the form factors is given for example in [11].

The total cross section for nonzero spin ($J \neq 0$) nuclei contains spin-independent and spin-dependent terms:

$$\begin{aligned}
\frac{d\sigma}{dq^2}(v, q^2) &= \frac{\Sigma |M|^2}{\pi v^2 (2J + 1)} = \frac{d\sigma_{\text{SI}}}{dq^2}(v, q^2) + \frac{d\sigma_{\text{SD}}}{dq^2}(v, q^2) = \\
&= \frac{\sigma_{\text{SI}}(0)}{4\mu_A^2 v^2} F_{\text{SI}}^2(q^2) + \frac{\sigma_{\text{SD}}(0)}{4\mu_A^2 v^2} F_{\text{SD}}^2(q^2),
\end{aligned}$$

where $\mu_A = \frac{m_\chi M_A}{m_\chi + M_A}$ is the reduced $\chi - A$ mass, $\sigma(0)$ is the cross section at zero-momentum transfer, $F(q^2)$ is a nuclear form factor, that is defined via nuclear structure functions. The spin-dependent (SD) part of the cross section at zero-momentum transfer takes the form $\sigma_{\text{SD}}(0) = \frac{4\mu_A^2}{\pi} \cdot \frac{J + 1}{J} (a_p \langle s_p^A \rangle + a_n \langle s_n^A \rangle)^2$,

where $\langle s_p \rangle = \langle N | s_p | N \rangle$ and $\langle s_n \rangle = \langle N | s_n | N \rangle$ are the expectation values of the spin content of the proton and neutron group in the nucleus. For many nuclei, detailed nuclear calculations have not been made and these parameters are dependent on the model.

The first model to estimate the spin content in the nucleus was independent single-particle shell model (SM) [12, 13]. There are several approaches to more accurate calculations: odd-group model (OGM) [14], its extended version [15], interacting boson–fermion model (IBFM) [16], etc. In table we collect the data for $\langle s_p \rangle$ and $\langle s_n \rangle$ for ^{73}Ge .

Zero-momentum spin structure of ^{73}Ge in different models

Models	$\langle s_p \rangle$	$\langle s_n \rangle$
ISPSM [18]	0	0.5
OGM [14, 15]	0	0.23
IBFM [16]	-0.009	0.469
IBFM (quenched) [16]	-0.005	0.245
TFFS [17]	0	0.34
SM (small) [12]	0.005	0.496
SM (large) [12]	0.011	0.498
Hybrid SM [13]	0.030	0.378

On the other hand, the coefficients a_p and a_n are parameterized in terms of the quark spin content of the proton and neutron $a_p = \sum_q A_q \Delta_q^p$, $a_n = \sum_q A_q \Delta_q^n$, where A_q is an axial-vector coupling from effective Lagrangian, and $\Delta_q^{p,n}$ can be extracted from data on polarized deep inelastic scattering. A global QCD analysis supplied us with the values

$$\Delta_u^p = \Delta_d^n = 0.78 \pm 0.02, \quad \Delta_d^p = \Delta_u^n = -0.48 \pm 0.02, \quad \Delta_s^p = \Delta_s^n = -0.15 \pm 0.02.$$

The spin-independent (SI) cross section takes the form

$$\sigma_{\text{SI}}(0) = \frac{4\mu_A^2}{\pi} (Z f_p + (A - Z) f_n)^2,$$

Z, A are atomic and mass numbers of the nucleus. In the limit $m_\chi \ll m_{\tilde{q}}$ the effective couplings of the lightest neutralino to protons and neutrons are approximated to

$$\frac{f_{p,n}}{m_{p,n}} = \sum_{q=u,s,d} f_{Tq}^{p,n} \frac{C_q}{m_q} + \frac{2}{27} f_{TG}^{p,n} \sum_{q=c,b,t} \frac{C_q}{m_q},$$

where $f_{Tq}^{p,n} = \frac{\langle n, p | m_q q \bar{q} | n, p \rangle}{m_{p,n}}$, $f_{TG}^{p,n} = 1 - \sum_{q=u,d,s} f_{Tq}^{p,n}$, and $f_{Tq}^{p,n}$ can be extracted from pion-nucleon sigma term.

It is useful to remember that there are significant theoretical uncertainties both from nuclear physics and from the spin content of the proton and neutron that enter into the cross section of elastic scattering of neutralino off the nuclei.

1.3. Event Rate. The elastic scattering of a relic neutralino from the target nucleus produces nuclear recoil E_R , which can be detected by a suitable detector. The differential event rate in respect to the recoil energy is the subject of experimental measurements. This differential event rate per unit mass of the target material has the form

$$\frac{dR}{dE_R} = N_T \frac{\rho_X}{m_X} \int_{v_{\min}}^{v_{\max}} dv f(v) v \frac{d\sigma}{dq^2}(v, q^2),$$

where $E_R = \frac{q^2}{2M_A}$ is typically about $10^{-6} m_\chi$, $N_T = \frac{N}{A}$ is a number density of target nuclei, N is Avogadro number. The direct detection rate integrated over the recoil energy interval from threshold energy ε till maximum energy e is a sum of SD and SI contributions:

$$R(\varepsilon, e) = \alpha(\varepsilon, e, m_\chi) \sigma_{\text{SI}}^p + \beta(\varepsilon, e, m_\chi) \sigma_{\text{SD}}^{pn},$$

where

$$\alpha(\varepsilon, e, m_\chi) = N_T \frac{\rho_X M_A}{2m_\chi \mu_p^2} A^2 A_{\text{SI}}(\varepsilon, e),$$

$$\beta(\varepsilon, e, m_\chi) = N_T \frac{\rho_X M_A}{2m_\chi \mu_p^2} \frac{4}{3} \frac{J+1}{J} (\langle s_p^A \rangle \cos \theta + \langle s_n^A \rangle \sin \theta)^2 A_{\text{SD}}(\varepsilon, e),$$

$$A_{\text{SI,SD}}(\varepsilon, e) = \frac{\langle v \rangle}{\langle v^2 \rangle} \int_{\varepsilon}^e dE_R F_{\text{SI,SD}}^2(E_R) I(E_R).$$

To estimate the event rate, one needs to know a number of quite uncertain astrophysical and nuclear structure parameters as well as the precise characteristics of the experimental set-up.

2. NUMERICAL RESULTS

2.1. Effective Low-Energy MSSM. To obtain as much as general predictions, it appeared more convenient to work within a phenomenological SUSY model, whose parameters are defined directly at the electroweak scale. Our MSSM

parameter space is determined by the entries of the mass matrices of neutralinos, charginos, Higgs-bosons, sleptons, and squarks. The list of the free parameters includes: $\text{tg}\beta$ — the ratio of neutral Higgs boson expectation values, μ — higgsino mass, $M_{1,2}$ — soft gaugino masses, M_A — CP-odd Higgs mass, $m_{\tilde{Q}}^2$, $m_{\tilde{U}}^2$, $m_{\tilde{D}}^2$, $m_{\tilde{L}}^2$, $m_{\tilde{E}}^2$ — squared squark (slepton) masses of the first and the second generation, $m_{\tilde{Q}_3}^2$, $m_{\tilde{T}}^2$, $m_{\tilde{B}}^2$, $m_{\tilde{L}_3}^2$, $m_{\tilde{\tau}}^2$ — squared squark (slepton) masses of the third generation, A_t , A_b , A_τ — soft trilinear couplings for the third generation, the third gaugino mass is defined as $M_2 = 0.3M_3$. We narrowed the intervals of the randomly scanned parameter space to the following:

$$\begin{aligned}
& -200 < M_1 < 200 \text{ GeV}, \quad -1 < M_2, \mu < 1 \text{ TeV} \\
& -2 < A_t < 2 \text{ TeV}, \quad 10 < \text{tg}\beta < 50, \\
& 50 < M_A < 500 \text{ GeV}, \quad 10 < m_{\tilde{Q},\tilde{Q}_3}^2, m_{\tilde{L},\tilde{L}_3}^2 < 10^6 \text{ GeV}^2, \\
& m_{\tilde{U}}^2 = m_{\tilde{D}}^2 = m_{\tilde{Q}}^2, \quad m_{\tilde{E}}^2 = m_{\tilde{L}}^2, \quad m_{\tilde{T}}^2 = m_{\tilde{B}}^2 = m_{\tilde{Q}_3}^2, \quad m_{\tilde{E}_3}^2 = m_{\tilde{L}_3}^2, \\
& A_b = A_\tau = 0.
\end{aligned}$$

The current experimental limits on sparticle and Higgs masses are included:

$$\begin{aligned}
& M_{\tilde{\chi}_{1,2}^\pm} \geq 100 \text{ GeV}, \quad M_{\tilde{\chi}_{1,2,3}^0} \geq 45, 76, 127 \text{ GeV}, \quad M_{\tilde{\nu}} \geq 43 \text{ GeV}, \\
& M_{\tilde{e}_R} \geq 70 \text{ GeV}, \quad M_{\tilde{q}} \geq 210 \text{ GeV}, \quad M_{\tilde{t}_1} \geq 85 \text{ GeV}, \\
& M_{H^0} \geq 100 \text{ GeV}, \quad M_{H^\pm} \geq 70 \text{ GeV}.
\end{aligned}$$

The calculations were made with the code based on [19], taking into account all the coannihilation channels with two-body final states that can occur between neutralinos, charginos, sleptons, stops and sbottoms, as long as their masses are $m_i < 2m_\chi$. We assume the relic density of light neutralinos $0.1 < \Omega_\chi h^2 < 0.3$ for cosmologically interesting region, $0.094 < \Omega_\chi h^2 < 0.129$ for WMAP prediction, $0.002 < \Omega_\chi h^2 < 0.1$ is correspondent to possibility that the LSP is not a unique DM candidate.

2.2. Cross Section for $m_\chi < 200$ GeV. For zero-spin nuclear target the experimentally measured event rate of direct DM particle detection is connected with zero-momentum WIMP–proton, –neutron cross sections, which can be expressed through effective neutralino–quark coupling. This coupling can be directly connected with the fundamental parameters of SUSY model. Thus the experimental limitations on spin-independent neutralino–nucleus cross section supply us with a constraint on the fundamental parameters of SUSY model. In the case of SD interaction the situation is similar, but we have in principle two constraints — for the neutralino–proton and neutralino–neutron effective spin couplings. In SD case there is a factorization of the nuclear structure for the zero-momentum-transfer cross section.

At first we calculated zero-momentum-transfer proton and neutron SI and SD cross sections in the effMSSM approach. The results are presented in Fig. 4. One can see that the largest cross section corresponds to the smallest values of Ω_χ .

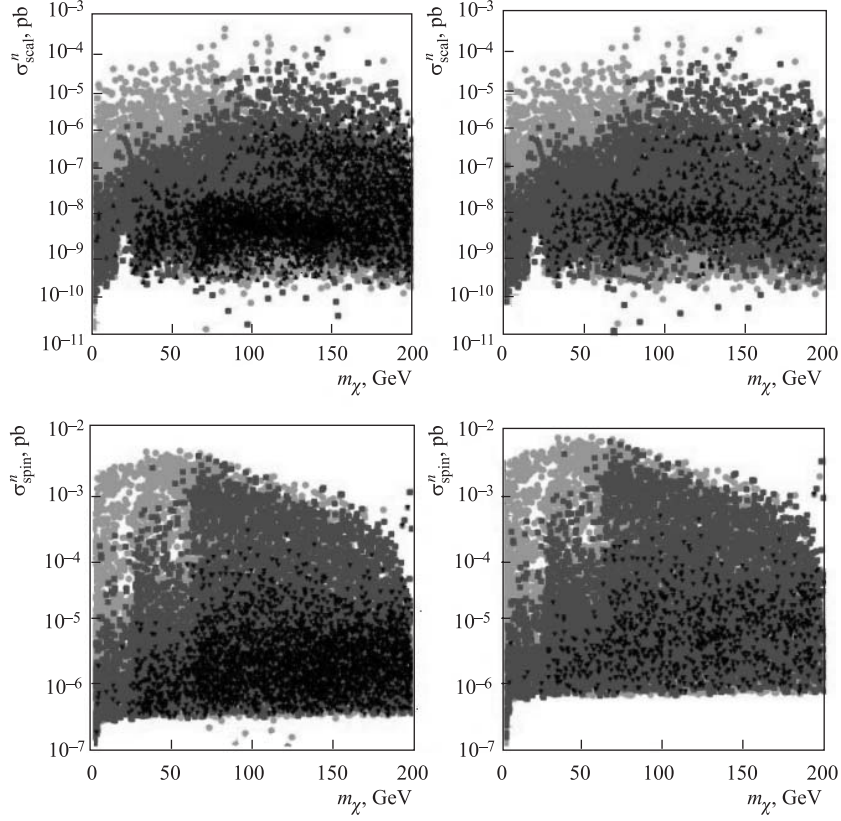


Fig. 4. Cross section of the spin-dependent and spin-independent interactions of WIMPs with the proton and neutron. Grey colour corresponds to the neutralino density $0 < \Omega_\chi h^2 < 1$, deep-grey colour corresponds to the subdominant relic neutralino contribution, black colour corresponds to the relic neutralino density in the left panel and to WMAP relic density in the right panel

In Figs. 5 and 6, the SD and SI cross sections as a function of the input MSSM parameters are presented. We can see the similar behaviour of the SD and SI cross sections as a function of μ and $m_{\tilde{Q}}^2$. There is no visible sensitivity of SD cross section to $\tan\beta$ and M_A , but SI cross section depends on these parameters. The value of SD cross section is about two orders of magnitude bigger, this fact is important for observations.

2.3. Constraints on WIMP–Nucleon Spin Interactions. There are a lot of models for calculation of the spin contents of nucleons (see above). In the earlier

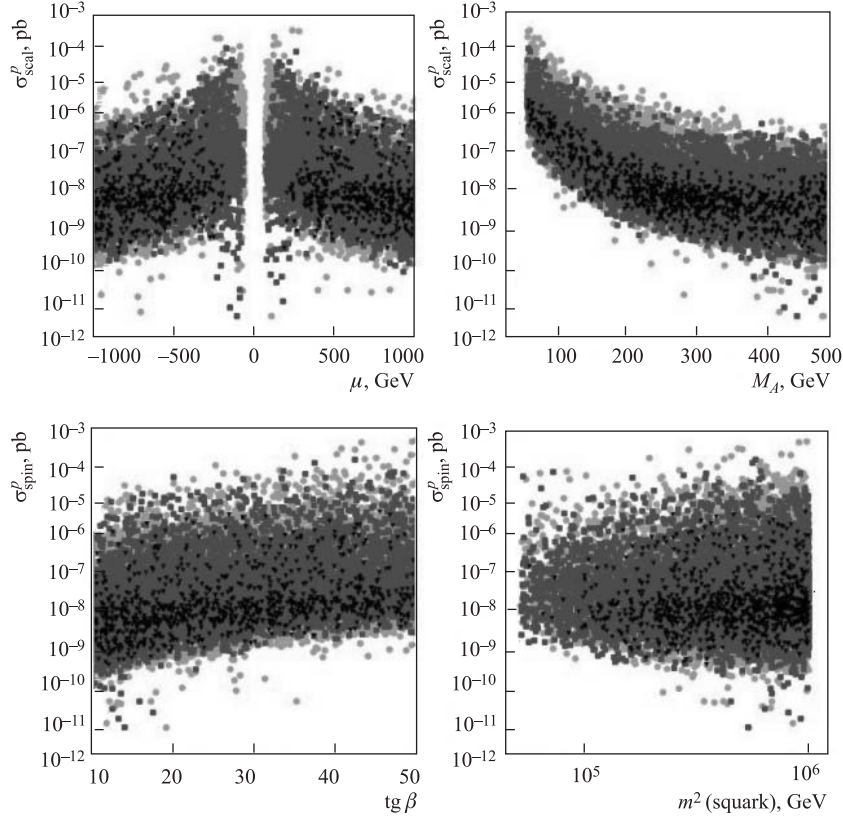


Fig. 5. Cross section of WIMP–proton spin-independent interactions as a function of input parameters of SUSY model with the same notations as in Fig. 4

consideration based on OGM one assumed that the nuclear spin is carried by the «odd» unpaired group of protons and neutrons and only one of either $\langle s_n^A \rangle$ or $\langle s_p^A \rangle$ is nonzero. The target nuclei can be classified into n -odd and p -odd groups. Further more accurate calculations of spin structure demonstrated that both $\langle s_n^A \rangle$ and $\langle s_p^A \rangle$ are nonzero, but one of the spin content is always dominant. If together with the dominance like $\langle s_{p(n)}^A \rangle \ll \langle s_{n(p)}^A \rangle$ one would have the WIMP–proton and WIMP–neutron couplings of the same order of magnitude ($a_p \sim a_n$), the situation could look like in OGM and one could neglect the subdominant spin contribution in the data analysis. For the case $a_{n(p)} \ll a_{p(n)}$ (proton and neutron contributions are strongly mixed) two new approaches appear in literature [20, 21].

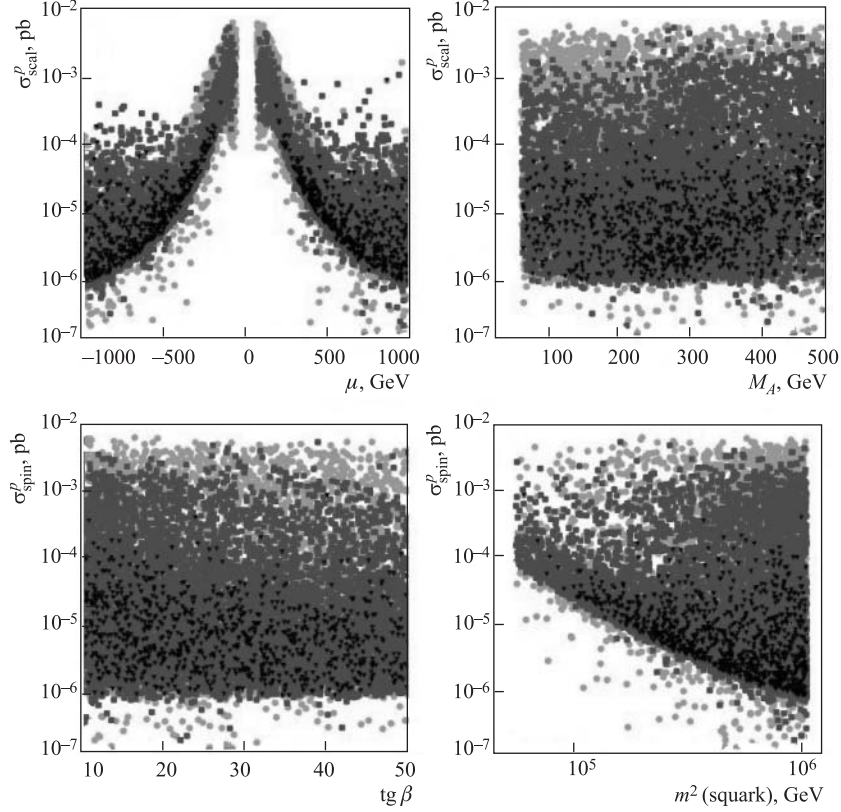


Fig. 6. Cross section of WIMP–proton spin-dependent interactions as a function of input parameters of SUSY model

For our investigations at first we compared WIMP–proton and WIMP–neutron couplings for $m_\chi < 200$ GeV, we obtained that $0.55 < |a_n/a_p| < 0.8$. Therefore, the couplings are the same and we can neglect, for example, $\langle s_p^A \rangle$ -spin contribution in our model. The results of our calculations and current experimental situation are presented in Figs. 7 and 8 for SD WIMP–proton and WIMP–neutron cross sections. The scatter plots for spin-dependent WIMP–proton cross section (Fig. 7) are obtained without any assumption about zero value of WIMP–neutron cross section ($\sigma_{\text{SD}}^n = 0$), but the experimental curves for WIMP–proton cross section σ_{SD}^p traditionally were extracted from the data under the full neglecting of the spin-neutron contribution. This one-spin-coupling dominance scheme allowed direct comparison of exclusion curves from different experiments.

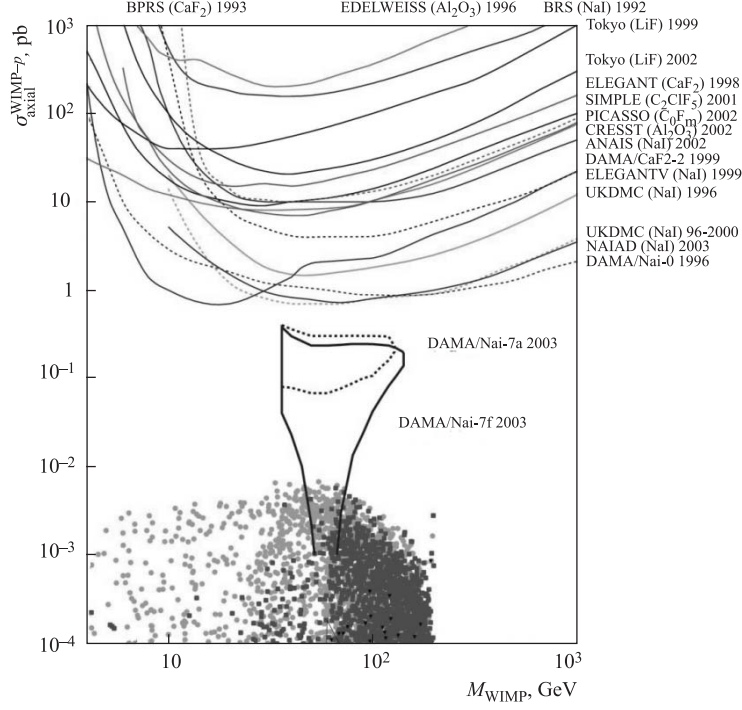


Fig. 7. Currently available exclusion curves for spin-dependent WIMP–proton cross sections. The scatter plots correspond to our calculations given in Figs. 4–6

In Fig. 7 curves for NAIAD and Tokyo-LiF experiments were calculated with subdominant contributions ($\sigma_{\text{SD}}^p \neq 0$, $\sigma_{\text{SD}}^n \neq 0$) [20]. One can see that this approach improves the sensitivity of these curves, but for reliable comparisons one should coherently recalculate all the previous curves in the new manner. For mixed spin–scalar coupling data presentation there is another approach [21]. It is based on an introduction of the so-called effective SD cross section:

$$\sigma_{\text{SD}}^{np} = \frac{\mu_p^2}{\pi} \frac{4}{3} [a_p^2 + a_n^2],$$

$$\sigma_{\text{SD}}^p = \sigma_{\text{SD}}^{pn} \cos^2 \theta, \quad \sigma_{\text{SD}}^n = \sigma_{\text{SD}}^{pn} \sin^2 \theta, \quad \text{tg } \theta = \frac{a_n}{a_p}.$$

In Figs. 7 and 8 the WIMP–nucleon spin and scalar mixed couplings allowed by the annual modulation signature from the 100 kg DAMA/NaI experiment are shown.

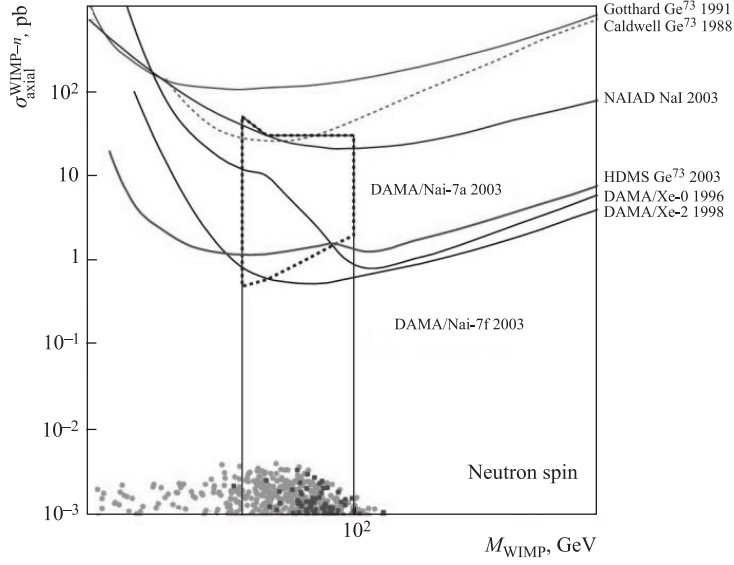


Fig. 8. Currently available exclusion curves for spin-dependent WIMP–neutron cross sections

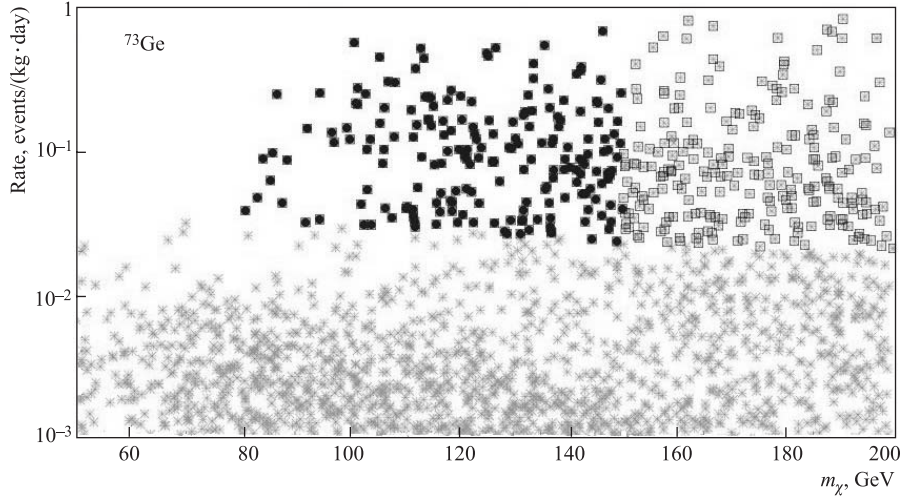


Fig. 9. Total event rate $R(0, \infty)$ for the direct neutralino detection in a ^{73}Ge detector as a function of the LSP neutralino mass. Crosses present our calculations with relic density constraint $0.1 < \Omega_{\tilde{\chi}} h^2 < 0.3$ only; open boxes, implementation of the DAMA SI cross section limit; closed boxes, results with additional WIMP-mass constraint

Comparing the number of exclusion curves in Figs. 7 and 8, one can see that there are many measurements with p -odd nuclei and there is a lack of data for n -odd nuclei. Therefore, measurements with n -odd nuclei are needed. This lack can be filled up with new data expected from HDMS experiment with high-spin isotope ^{73}Ge [22]. One-order-of-magnitude improvement of the HDMS sensitivity will supply us with the best exclusion curve for SD WIMP–neutron coupling, but this sensitivity is not yet enough to reach the calculated upper bound for σ_{SD}^n .

2.4. Some Consequences of the DAMA Results. The main results of the DAMA experiment are the limitation of the WIMP mass and the restrictions on

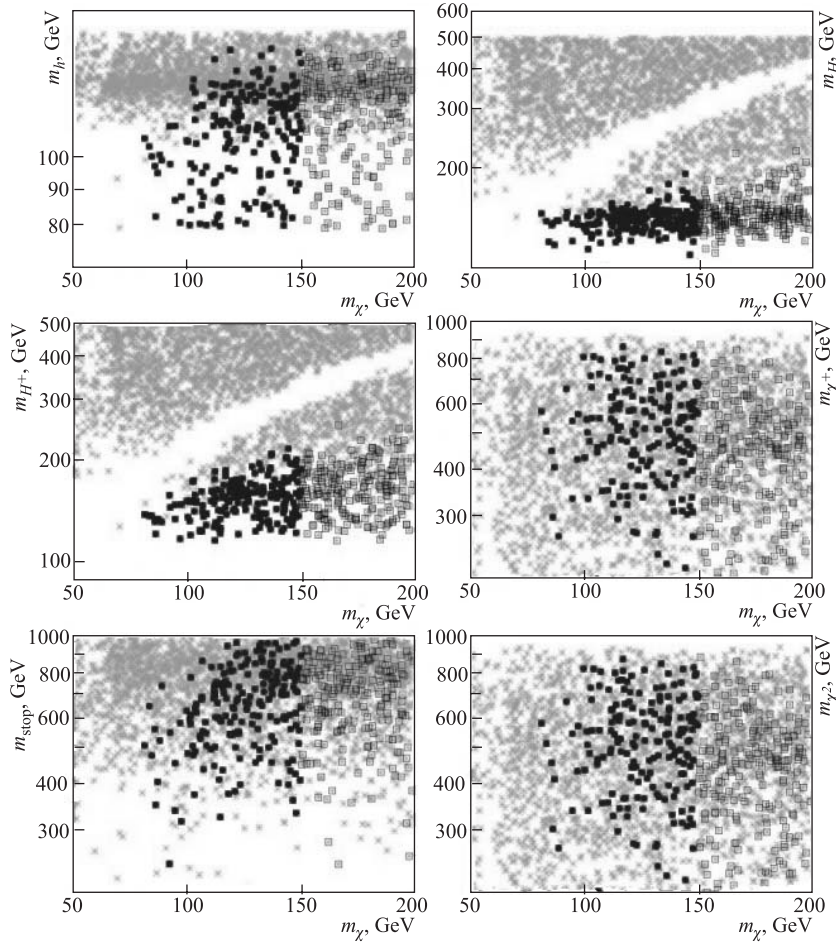


Fig. 10. Masses in GeV of light, heavy and charged Higgs bosons, chargino, stop quark, and second neutralino versus the mass of the LSP neutralino under the DAMA restrictions

the cross section of the scalar WIMP–proton interaction:

$$40 < m_{\text{WIMP}} < 150 \text{ GeV}, \quad 1 \cdot 10^{-7} < \sigma_{\text{SI}}^p(0) < 3 \cdot 10^{-5} \text{ pb}.$$

Taking these limitations into account, we have obtained the reduction of our scatter plots for the total expected event rate of direct WIMP detection in a ^{73}Ge detector (Fig. 9) and the indirect detection rate for upgoing muons from dark-matter particles annihilation on the Earth and on the Sun (Fig. 11). There is also a reduction of allowed masses of some SYSU particles (Fig. 10).

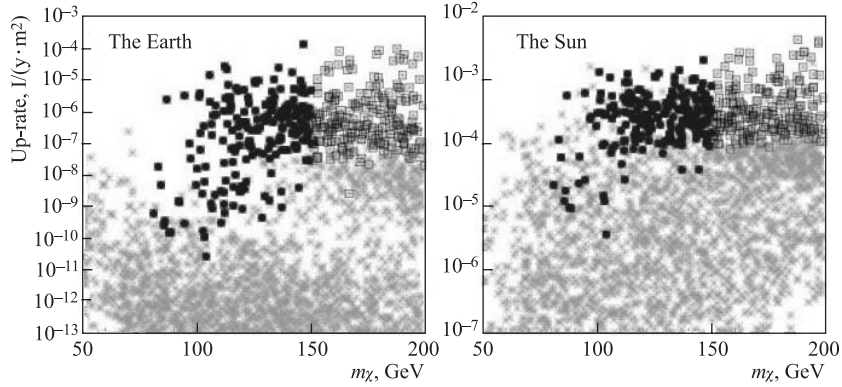


Fig. 11. Indirect rate for upgoing muons from neutralino annihilation on the Earth (left) and on the Sun (right) with the same notations as in Fig. 9

One can see that the DAMA evidence favours the light Higgs sector of the MSSM, relatively high event rate in Ge detectors, as well as relatively high up going muon fluxes from the Earth and from the Sun for indirect detection of the relic neutralino. It is also almost insensitive to the sfermion and neutralino–chargino particle masses. The light Higgs masses (smaller than 200 GeV) are very interesting from the viewpoint of accelerator SUSY searches.

CONCLUSIONS

In the effective low-energy MSSM for zero-momentum transfer we calculated the LSP–proton, –neutron spin and scalar cross sections in the low LSP mass regime $40 < m_{\text{WIMP}} < 150 \text{ GeV}$, which follows from the DAMA dark matter evidence. We compared the calculated cross sections with experimental exclusion curves and demonstrated that about a two orders of magnitude improvement of the current DM experiment sensitivities is needed to reach the SUSY predictions for the WIMP–proton, WIMP–neutron spin-dependent cross sections.

The DAMA evidence favours the light Higgs sector in the effMSSM, which could be reached at LHC, a high event rate in a ^{73}Ge detector and relatively high upgoing muon fluxes from relic neutralino annihilations on the Earth and the Sun.

REFERENCES

1. *Bernabei R. et al.* // Phys. Lett. B. 2000. V. 480. P. 23.
2. *Bernabei R. et al.* // Riv. Nuovo Cim. 2003. V. 26. P. 1; astro-ph/0307403.
3. *Bernabei R. et al.* // astro-ph/0311046.
4. *Klapdor-Kleingrothaus H. V. et al.* // Nucl. Instr. Meth. A. 2003. V. 511. P. 341; hep-ph/0309170.
5. *Tomei C. et al.* // Nucl. Instr. Meth. A. 2003. V. 508. P. 343; hep-ph/0306257.
6. *Bednyakov V. A. et al.* // Phys. Lett. B. 1994. V. 329. P. 5; hep-ph/9401271.
7. *Engel J.* // Phys. Lett. B. 1991. V. 264. P. 114.
8. *Bednyakov V. A., Klapdor-Kleingrothaus H. V.* hep-ph/0404102.
9. *Harber H. E.* // Phys. Rep. 1985. V. 117. P. 75.
10. *Gunion J. F.* // Nucl. Phys. B. 1986. V. 272. P. 1.
11. *Jungman G. et al.* // Phys. Rep. 1996. V. 267. P. 195.
12. *Goodman M. V., Witten E.* // Phys. Rev. D. 1985. V. 31. P. 3059.
13. *Dimitrov V. et al.* // Phys. Rev. D. 1995. V. 51. P. 291.
14. *Engel J., Vogel P.* // Phys. Rev. D. 1989. V. 40. P. 3132.
15. *Engel J. et al.* // Int. J. Mod. Phys. E. 1992. V. 1. P. 1.
16. *Iachello F. et al.* // Phys. Lett. B. 1991. V. 254. P. 220.
17. *Nikolaev M. A., Klapdor-Kleingrothaus H. V.* // Z. Physik. A. 1993. V. 345. P. 373.
18. *Ellis J. R., Flores R. A.* // Nucl. Phys. B. 1988. V. 307. P. 883.
19. *Bednyakov V. A. et al.* // Phys. Rev. D. 2002. V. 66. P. 115005, 015010.
20. *Tovey D. R. et al.* // Phys. Lett. B. 2000. V. 488. P. 17.
21. *Bernabei R. et al.* // Phys. Lett. B. 2001. V. 509. P. 197.
22. *Klapdor-Kleingrothaus H. V. et al.* // Astropart. Phys. 2003. V. 18. P. 525.

Received on August 20, 2004.

Редактор *Н. С. Скокова*
Макет *Е. В. Сабоевой*

Подписано в печать 14.10.2004.
Формат 60 × 90/16. Бумага офсетная. Печать офсетная.
Усл. печ. л. 1,25. Уч.-изд. л. 1,81. Тираж 360 экз. Заказ № 54627.

Издательский отдел Объединенного института ядерных исследований
141980, г. Дубна, Московская обл., ул. Жолио-Кюри, 6.
E-mail: publish@pds.jinr.ru
www.jinr.ru/publish/